ELSEVIER

Journal of Molecular Structure 510 (1999) 59–68

Journal of
MOLECULAR
STRUCTURE

www.elsevier.nl/locate/molstruc

An ab initio and matrix isolation infrared study of the 1:1 C_2H_2–$CHCl_3$ adduct

E.D. Jemmis[a], K.T. Giju[a], K. Sundararajan[b], K. Sankaran[b], V. Vidya[b], K.S. Viswanathan[b,*], J. Leszczynski[c]

[a]*School of Chemistry, University of Hyderabad, Hyderabad 500 046, India*
[b]*Materials Chemistry Division, Indira Gandhi Centre for Atomic Research, Kalpakkam 603 102, India*
[c]*Department of Chemistry, Jackson State University, Jackson, MS 39217, USA*

Received 6 November 1998; accepted 12 January 1999

Abstract

The details of weak C–H$\cdots\pi$ interactions that control several inter and intramolecular structures have been studied experimentally and theoretically for the 1:1 C_2H_2–$CHCl_3$ adduct. The adduct was generated by depositing acetylene and chloroform in an argon matrix and a 1:1 complex of these species was identified using infrared spectroscopy. Formation of the adduct was evidenced by shifts in the vibrational frequencies compared to C_2H_2 and $CHCl_3$ species. The molecular structure, vibrational frequencies and stabilization energies of the complex were predicted at the MP2/6-311+G(d,p) and B3LYP/6-311+G(d,p) levels. Both the computational and experimental data indicate that the C_2H_2–$CHCl_3$ complex has a weak hydrogen bond involving a C–H$\cdots\pi$ interaction, where the C_2H_2 acts as a proton acceptor and the $CHCl_3$ as the proton donor. In addition, there also appears to be a secondary interaction between one of the chlorine atoms of $CHCl_3$ and a hydrogen in C_2H_2. The combination of the C–H$\cdots\pi$ interaction and the secondary Cl$\cdots$H interaction determines the structure and the energetics of the C_2H_2–$CHCl_3$ complex. In addition to the vibrational assignments for the C_2H_2–$CHCl_3$ complex we have also observed and assigned features owing to the proton accepting C_2H_2 submolecule in the acetylene dimer. © 1999 Elsevier Science B.V. All rights reserved.

Keywords: Ab initio calculations; Matrix isolation; Infrared spectroscopy; Acetylene; Chloroform

1. Introduction

The importance of intermolecular interactions in biology and material science has prompted chemists in recent years to explore the variety of such interactions. There has, therefore, been a tremendous surge in the study of supramolecular chemistry during the last decade [1]. The strongest of these interactions are the hydrogen bonds involving an acidic hydrogen and an electronegative atom bearing one or more lone pairs of electrons [2]. Recently π-electrons have been shown to act as electron donors in hydrogen bonding with H–X groups, where X = N or O [3–7]. The strength of such interaction should decrease further when X stands for carbon. Despite the extremely weak binding, several examples are now known where relatively nonpolar C–H interacts with π-electrons [8–14]. It has been suggested that the cooperative C–H$\cdots\pi$ hydrogen bonds are the main reason for the existence of large number of short C–H$\cdots\pi$

* Corresponding author. Tel.: + 91-4114-40398; fax: + 91-4114-40365.
E-mail address: vish@igcar.ernet.in (K.S. Viswanathan)

0022-2860/99/$ - see front matter © 1999 Elsevier Science B.V. All rights reserved.
PII: S0022-2860(99)00027-7

contacts, observed primarily from the X-ray structure data [15,16–19]. Such a phenomena generates the following questions: What is the strength of the individual C–H$\cdots\pi$ interactions? What is the contribution of the cooperativity effect to the overall interaction scenario? In the condensed phase, the cooperativity effect cannot be avoided and isolated molecule techniques are necessary to study such interactions involving individual C–H$\cdots\pi$ contacts.

We present here a study of the interaction of C_2H_2 with $CHCl_3$ using matrix isolation infrared spectroscopy, and post-Hartree–Fock ab initio MO and hybrid density functional theory methods. A variety of complexes of acetylene have been reported in the literature, and it has been shown that acetylene can act both as a proton donor and a proton acceptor [20–22]. For example, in acetylene–hydrogen halide complexes, the hydrogen halides are the proton donors and acetylene the proton acceptor [22]. The interactions in these cases were of the H$\cdots\pi$ variety. A number of C–H$\cdots\pi$ complexes have also been reported in the literature, involving ethylenic and aromatic systems [23–29]. However, in the acetylene–water complex, acetylene is the proton donor [20]. Similarly chloroform has also been shown to interact both as a proton donor or a proton acceptor. Interactions between $CHCl_3$ and HF result in two types of hydrogen bonded complexes, one involving the hydrogen of HF and another involving the hydrogen of $CHCl_3$ [30]. In the solid state gold derivatives of acetylene are found to form 1:2 and 1:4 complexes with $CHCl_3$ [13]. The enhanced charge at π bonds of the metal acetylide facilitates this C–H$\cdots\pi$ interaction. There is no experimental evidence for the C_2H_2–$CHCl_3$ complex so far. In earlier studies on the $CHCl_3$-triethyl phosphate complex, we have shown that $CHCl_3$ acts as a Lewis acid [31]. It was therefore thought interesting to extend such study to the C_2H_2–$CHCl_3$ complex in order to better understand the nature of such specific interaction.

2. Experimental

A Leybold Heraeus closed cycle helium compressor cooled cryostat was used to attain the low temperature ($\approx$12 K) required for the matrix isolation experiments. The cryostat was housed in a vacuum chamber where the base pressure was $< 10^{-6}$ torr. The details of the vacuum system and the related experimental setup, have been described elsewhere [32].

Acetylene (commercial grade, Asiatic Oxygen Limited, India) was chilled to temperatures of about $\approx$170 K, and then pumped to eliminate volatile impurities. Chloroform (Spectrosol grade, BDH) was used without any further purification. Acetylene and the matrix gas, argon (IOLAR grade 1), were mixed in the desired ratios using standard manometric procedures. This gas mixture was then streamed through an effusive nozzle. Vapors of chloroform, at a suitable flow rate were simultaneously streamed through another nozzle, so that the $Ar/C_2H_2/CHCl_3$ mixture, of the desired composition, was deposited on a KBr substrate mounted on a cryotip. We used matrix to sample ratios ranging from 3000:1 to 3000:0.1 for acetylene and 3000:2 to 3000:10 for chloroform. Deposition rates employed were $\approx$3 mmol/h, and a deposition typically lasted for about 30 min.

Infrared spectra of the matrix isolated samples were recorded over the range 4000 to 400 cm^{-1}, using a BOMEM MB 100 FTIR spectrometer, operated at a resolution of 1 cm^{-1}. The matrix was then annealed by warming it to 35 K, maintained at this temperature for about 15 min and then recooled to 12 K. Spectra of the matrix, thus annealed, were then recorded. All spectra shown in this paper were those recorded after annealing the matrix. Spectra were also recorded where acetylene and chloroform were deposited separately.

3. Theoretical methods

The fully optimized geometries of the C_2H_2, $CHCl_3$ and the C_2H_2–$CHCl_3$ adduct were calculated using the GAUSSIAN 92/DFT [33] and GAUSSIAN 94 [34] packages. MP2 [35] and B3LYP [36–39] levels of theory, in conjunction with 6-311+G(d,p) basis sets [40] were applied in this study. The hybrid Hartree–Fock density functional method, B3LYP, uses the Becke's three parameter non-local exchange functional [36,37], with the non-local correlation functional of Lee et al. [38].

The vibrational frequency calculations were

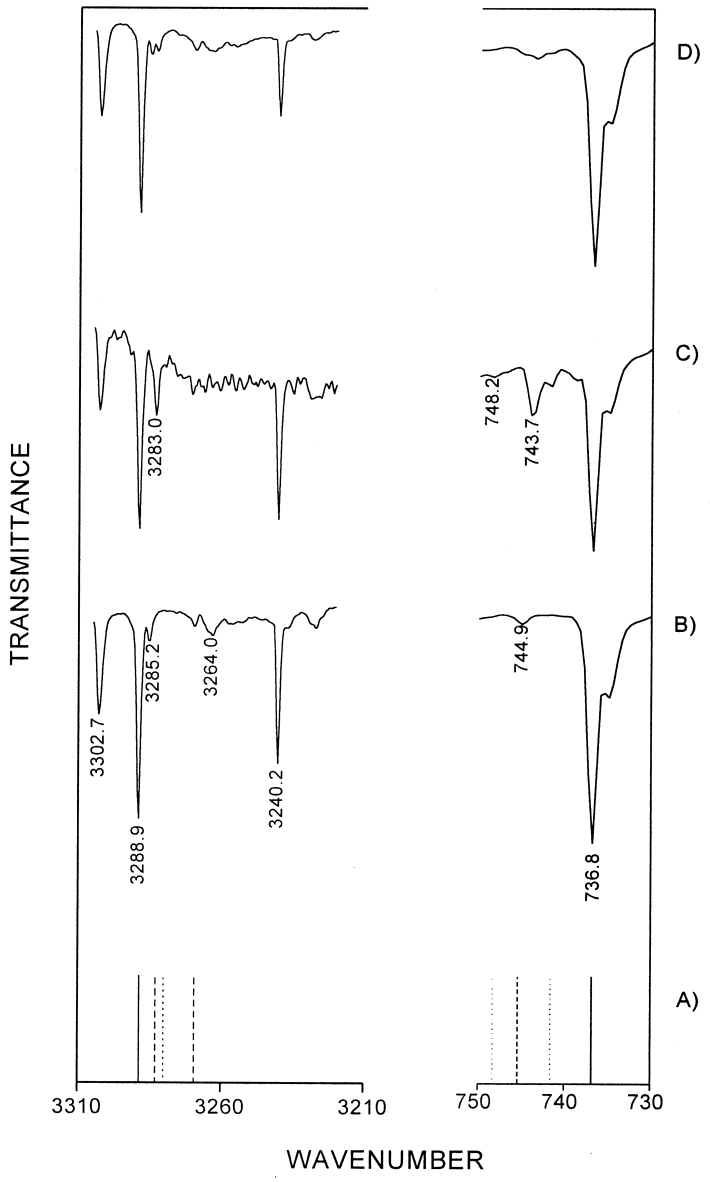

Fig. 1. Matrix isolation infrared spectra in the region 3310–3210 cm^{-1} and 750–730 cm^{-1}: (a) computed stick spectra; (b) C_2H_2/Ar (1:3000); (c) $C_2H_2/CHCl_3$/Ar (0.1:10:3000); (d) $C_2H_2/CHCl_3$/Ar (1:2:3000). In the stick spectra, solid lines denote features of C_2H_2 monomer, short dashes C_2H_2 dimer, and dotted line C_2H_2–$CHCl_3$ complex.

performed numerically at the MP2 level and analytically at the B3LYP level, for the reference geometries optimized at the same level of theory. Vibrational frequency calculations enabled us to characterize the nature of the stationary points, and also to assign the experimental frequencies of vibrational modes recorded for the complex. Since MP2 level gave one very small imaginary frequency (4i) (probably owing to the drawback of a numerical calculation), we have chosen the analytical frequencies of B3LYP level for comparison with the frequency values obtained from the matrix isolation spectra.

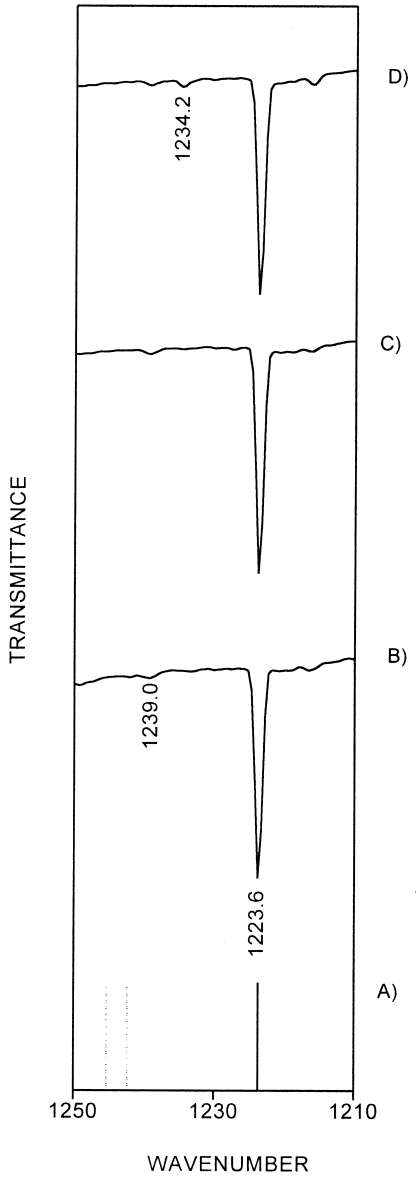

Fig. 2. Matrix isolation infrared spectra in the region 1250–1210 cm^{-1}: (a) computed stick spectra; (b) $CHCl_3$/Ar (6:3000); (c) C_2H_2/$CHCl_3$/Ar (0.1:10:3000); (d) C_2H_2/$CHCl_3$/Ar (1:2:3000). In the stick spectra, solid lines denote feature of $CHCl_3$, and dotted lines C_2H_2–$CHCl_3$ complex.

The predicted interaction energies were corrected for zero-point vibrational energy (ZPE) and basis set superposition error using counterpoise method of Boys and Bernardi [41].

4. Results and discussion

4.1. Experimental

Fig. 1 shows the spectra obtained when acetylene and chloroform were codeposited in an argon matrix. Also shown in this figure, is the spectrum obtained when acetylene alone was deposited in an argon matrix. The region spanned in this figure is that between 3310–3210 cm^{-1} and 750–730 cm^{-1}. In these spectral regions, C_2H_2 has strong absorptions at 3288.9, 3302.7 and at 736.8 cm^{-1}, which have been assigned to the ν_3, combination band $\nu_2 + \nu_4 + \nu_5$, and ν_5 modes respectively, of C_2H_2 [42]. Chloroform has no absorptions in these regions.

When acetylene and chloroform were codeposited and the matrix then annealed, product absorption band appeared at 3283.0, 748.2 and 743.7 cm^{-1}. These bands appeared only when both the reagents were codeposited. Further, these bands increased in intensity as the concentration of either of the two reagents were increased. These observations clearly indicate that these features are the result of a complex involving chloroform and acetylene. Since these product bands appeared at low concentrations of acetylene and chloroform, we believe that these bands are the result of a 1:1 complex of acetylene and chloroform.

The feature at 3283.0 cm^{-1} can be assigned to the ν_3 mode of the C_2H_2 submolecule in the C_2H_2–$CHCl_3$ complex. This assignment implies that following complex formation, the ν_3 mode of the C_2H_2 submolecule is redshifted by 5.9 cm^{-1} from the value obtained for free C_2H_2 for this mode.

The features at 743.7 and 748.2 cm^{-1} can be assigned to the ν_5 mode of the C_2H_2 submolecule in the C_2H_2–$CHCl_3$ complex. The ν_5 mode in the free C_2H_2 molecule is a doubly degenerate (π_u) mode which on complex formation splits into two components owing to the loss of the cylindrical symmetry of the C_2H_2 submolecule.

We also observed spectral features of C_2H_2 dimer at 3264.0 cm^{-1} [42], and that of the C_2H_2–H_2O complex at 3240.2 and 790.0 cm^{-1} [20], in excellent agreement with those reported in the literature. Features of the water complex appear, as water is an inevitable impurity in the matrix isolation experiments.

Fig. 2 shows the infrared spectra over the region 1250 to 1210 cm^{-1} where the C–H bending of $CHCl_3$

Table 1
Experimental and computed (scaled) frequencies, scaling factors and mode assignments for the C_2H_2–$CHCl_3$ adduct

Experiment ν (cm^{-1})	Calculated ν (cm^{-1})	Scaling factor	Mode assignmnet
3288.9	3288.3 (93)[a]	0.961	ν_3 of C_2H_2
3283.0	3280.3 (97)	0.961	ν_3 of C_2H_2 in C_2H_2–$CHCl_3$
3285.2	3282.8 (99)	0.961	ν_3 of C_2H_2 in C_2H_2 dimer[b]
3264.0	3269.5 (169)	0.961	$\nu_3$of C_2H_2 in C_2H_2 dimer[c]
736.8	736.3 (111)	0.953	ν_5 of C_2H_2
743.7, 748.2	741.2 (113) 747.8 (123)	0.953	ν_5 of C_2H_2 in C_2H_2–$CHCl_3$
744.9	736.4 (44) 744.9 (121)	0.953	ν_5 of C_2H_2 in C_2H_2 dimer[b]
757.6	754.1 (154) 759.6 (85)	0.953	ν_5 of C_2H_2 in C_2H_2 dimer[c]
1223.6	1223.8 (28)	0.982	ν_4 of $CHCl_3$
1234.2	1241.8 (34) 1245.1 (34)	0.982	ν_4 of $CHCl_3$ in C_2H_2–$CHCl_3$[d]

[a] Computed infrared intensities (KM/mole) are given in parenthesis.
[b] Mode involving C_2H_2 as a proton acceptor.
[c] Mode involving C_2H_2 as a proton donor.
[d] Unscaled lowest frequencies (cm^{-1}) of the C_2H_2–$CHCl_3$ adduct are 16.2, 28.1, 28.3, 55.9, and 78.3 with negligible intensities.

(ν_4) is observed. This mode is recorded at 1223.6 cm^{-1} in free $CHCl_3$ and at 1234.2 cm^{-1} in the C_2H_2–$CHCl_3$ complex. Complex formation has therefore resulted in a 10.6 cm^{-1} blue shift for this mode. As mentioned earlier, the peak at 1234.2 cm^{-1} was attributed to the C_2H_2–$CHCl_3$ complex, as this spectral feature appeared only when both the reagents were codeposited. Experiments with $CDCl_3$ and C_2H_2 were also carried out to observe the isotopic shifts in this mode. However, the ν_4 mode of free $CDCl_3$ showed a severe multiplet splitting, owing to matrix site effects. The complex nature of the spectral features of free $CDCl_3$ made it impossible for us to discern the features corresponding to this mode in the C_2H_2–$CDCl_3$ complex.

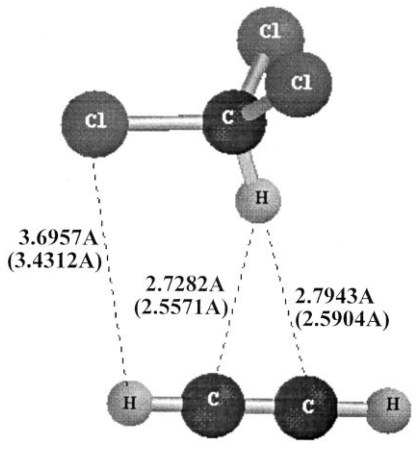

Fig. 3. Optimized structure of the C_2H_2–$CHCl_3$ complex computed at the B3LYP/6-311+G(d,p) level. Values in parentheses are at the MP2/6-311+G(d,p) level.

No feature corresponding to the C–H stretch in the $CHCl_3$ submolecule could be observed, probably because its intensity may have been too low to be discerned. The ν_1, ν_2 and ν_4 modes in C_2H_2 which are infrared inactive in the free molecule, may be expected to become infrared active in the complex, following the lowering of the symmetry in the complex. However, none were observed, probably because the interaction in this complex is too weak to cause any significant perturbations in these modes. This conclusion is borne out by our computations, which indicate only an insignificant infrared intensity for these modes. In addition our experimental set-up did not permit the measurement of the five new very low frequency vibrational modes generated as a consequence of the complex formation. Calculated frequencies for these modes are listed in Table 1.

4.2. Structure of the C_2H_2–$CHCl_3$ complex and interaction energies

The results of our computations indicated that a complex involving a C–H$\cdots\pi$ interaction between C_2H_2 and $CHCl_3$, as shown in Fig. 3, corresponded to a minimum on the potential surface. The structural parameters and charges on the different atoms in the

Table 2
Bond distances (Å) and angles (in degrees) for the C_2H_2–$CHCl_3$ complex

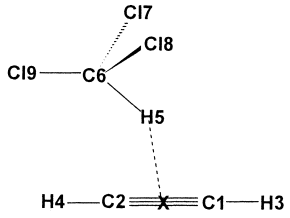

Parameter	MP2/6-311+G(d,p)	B3LYP/6-311+G(d,p)
C1–H3	1.0658 (1.0645)[a]	1.0638 (1.0630)
C1–C2	1.2175 (1.2162)	1.1999 (1.1993)
C2–H4	1.0660 (1.0645)	1.0640 (1.0630)
C6–H5	1.0836 (1.0848)	1.0835 (1.0821)
C6–Cl7	1.7650 (1.7652)	1.7867 (1.7863)
C6–Cl9	1.7678 (1.7652)	1.7904 (1.7863)
X–H5	2.5010	2.6955
C1–H5	2.5904	2.7943
C2–H5	2.5571	2.7282
C2–C6	3.5147	3.7127
C2–Cl9	3.7556	4.0160
H4–C6	3.7123	3.8885
H4–Cl9	3.4312	3.6957
∠C2–C1–H3	179.2 (180.0)	179.3 (180.0)
∠C2–C1–H4	179.8 (180.0)	179.8 (180.0)
∠H5–C6–Cl7	107.8 (107.6)	107.9 (107.5)
∠H5–C6–Cl9	107.1 (107.6)	107.2 (107.5)
∠Cl7–C6–Cl8	111.4 (111.3)	111.3 (111.4)
∠Cl7–C6–Cl9	111.2 (111.3)	111.2 (111.4)
∠X–H5–C6	160.6	163.6
∠C1–X–H5	91.6	93.2
∠C2–X–H5	88.4	86.8
∠H3–C1–H5	106.0	106.4
∠H4–C2–H5	101.9	99.6

[a] Here, wherever relevant, the structural parameters for the uncomplexed species are given in parentheses.

Table 3
Atomic charges on the various atoms of the C_2H_2–$CHCl_3$ complex at different levels of theory using the Mulliken scheme

Atom	MP2/6-311+G(d,p)	B3LYP/6-311+G(d,p)
C1	−0.2892 (−0.1797)[a]	−0.2370 (−0.1560)
C2	−0.0769 (−0.1797)	−0.0733 (−0.1560)
H3	0.1829 (0.1797)	0.1586 (0.1560)
H4	0.1899 (0.1797)	0.1629 (0.1560)
H5	0.3172 (0.2903)	0.3311 (0.3121)
C6	−0.6686 (−0.7442)	−0.8036 (−0.8550)
Cl7	0.1285 (0.1513)	0.1677 (0.1810)
Cl8	0.1285 (0.1513)	0.1677 (0.1810)
Cl9	0.0877 (0.1513)	0.1260 (0.1810)

[a] The atomic charges on the atoms for the uncomplexed species is given in parenthesis.

complex are shown in Tables 2 and 3 respectively, computed at both MP2/6-311+G(d,p) and B3LYP/6-311+G(d,p) levels of theory. The distance between the hydrogen in $CHCl_3$ and the centre of the π bond in C_2H_2, (X–H5 distance in Table 2), is 2.696 Å at the B3LYP level and 2.501 Å at the MP2 level. These are to be compared to the MP2/6-31G(d) (2.622 Å) and DFT (2.168 Å) results reported by Mingos et al. [14]. The shorter distance of 2.501 Å at the MP2 level is comparable to the experimental values found for the derivatives of AuC≡CAu [13]. In addition to this interaction, our calculations also indicate another possibly weaker interaction, between one of the chlorines (Cl9) in $CHCl_3$ and a hydrogen (H4) in C_2H_2. The distance between these two atoms is 3.696 Å at the B3LYP level, which is within the known intermolecular contacts of 2.8–4.0 Å, for this pair of atoms [43,44]. It is possible that this secondary interaction causes a tilt of the C–Cl bond in $CHCl_3$ towards acetylene, as seen in Fig. 3. Thus, the combined interaction determines the structure and the energies of the complex.

Table 4 gives the total energies and the zero-point vibrational energies of the submolecules and the complexes. Table 5 gives interaction energies for the adduct formation. Formation of the acetylene–chloroform adduct is exothermic by 1.82 kcal/mol at the MP2 level after counterpoise correction. ZPE corrections reduce this to 1.52 kcal/mol. Corresponding values at the B3LYP level are 1.19 and 0.79 kcal/mol respectively. The lower interaction energies reported by Mingos et al. should be the result of smaller basis set used in that study [14]. However these are considerably larger than the dimerization energy of acetylene (0.68 and 0.38 kcal/mol respectively at the B3LYP level). This is in tune with vibrational frequency shifts. The greater stability of the C_2H_2–$CHCl_3$ complex compared with the C_2H_2 dimer stems from the nature of the interaction in the two systems. The C_2H_2 dimer is stabilized only via a C–H$\cdots\pi$ interaction, while the C_2H_2–$CHCl_3$ is stabilized by dual interactions as discussed earlier.

The existence of these interactions can also be inferred from an examination of the net atomic

Table 4
Total energy (hartrees) and zero point vibrational energy (kcal/mol) at MP2/6-311+G(d,p)//MP2/6-311+G(d,p) and B3LYP/6-311+G(d,p)//B3LYP/6-311+G(d,p) levels. The number of imaginary frequencies (NIM) is given in parenthesis

Molecule	MP2		B3LYP	
	Total energy	ZPE (NIM)	Total energy	ZPE (NIM)
C_2H_2	−77.11323	16.6 (0)	−77.35665	17.0 (0)
$CHCl_3$	−1417.52730	13.0 (0)	−1419.37967	12.4 (0)
C_2H_2–$CHCl_3$	−1494.64654	29.9 (1)[a]	−1496.73866	29.8 (0)
C_2H_2–C_2H_2	−152.22946	33.8 (0)	−154.71460	34.3 (0)

[a] Value of this imaginary frequency is 4i.

charges on the atoms in the complex compared with the values in the uncomplexed species. For example, the H5 in chloroform involved in the H–π bonding, shows an increase of ≈6% in its charge in the complex, compared with that in free chloroform. Such an increase in the atomic charge of the hydrogen involved in H-bonding is typical [45,46]. The secondary interaction involving the Cl of $CHCl_3$ and H in C_2H_2 is indicated by changes in atomic charges. The Cl9 involved in this interaction shows large decrease in its charge (by ≈30%), whereas the other chlorines not participating in this interaction show insiginificant changes in their charges. Likewise, H4 also shows a ≈4% increase in its charge in the complex, while the other hydrogen in C_2H_2 shows a negligible change.

In the earlier discussions, we have examined the *changes* in the atomic charges, computed using the Mulliken scheme. It must be noted that at the level of theories referred earlier, the net charge on chlorine was indicated to be positive (Table 3), possibly owing to basis set effects and the scheme adopted to compute charges. This point was confirmed, as a single point calculation at the B3LYP/AUG-cc-pVTZ level, using the geometry optimized at the B3LYP/6-311+G(d,p) level, revealed that the Mulliken charges on chlorines were indeed negative when the basis set was changed. Likewise, computation of charges at the B3LYP/6-311+G(d,p) level using the chelpg scheme of Breneman yielded charges on chlorines that were slightly negative.

4.3. Vibrational assignments

Vibrational frequencies of the different modes were calculated for this complex and compared with the experimentally observed values (Table 1). The computed frequencies for the different modes were scaled on a mode-by-mode basis, by comparing these frequencies for the uncomplexed C_2H_2 or $CHCl_3$ with those obtained experimentally. The scaling factors thus obtained for the different modes of the uncomplexed reagents were then used to scale the computed frequencies in the complex. Such a mode-by-mode scaling is warranted as the different vibrational modes in the complex may be perturbed differently by the matrix. The scaling factors for the different modes are also given in the table. It can be seen that the scaled computed frequencies agree with those obtained experimentally both in magnitude and direction. The computed frequencies have also been shown as a stick spectra in both Figs. 1 and 2, to

Table 5
Interaction energies (kcal/mol) calculated at MP2/6-311+G(d,p) and B3LYP/6-311+G(d,p) levels

Reaction	MP2		B3LYP	
	E_{CP}[a]	E_{CP} + ZPE[b]	E_{CP}[a]	E_{CP} + ZPE[b]
$C_2H_2 + CHCl_3 \rightarrow C_2H_2$–$CHCl_3$	− 1.82	− 1.52	− 1.19	− 0.79
$2\ C_2H_2 \rightarrow C_2H_2$–$C_2H_2$	− 1.05	− 0.45	− 0.68	− 0.38

[a] E_{CP}: interaction energy corrected for counterpoise.
[b] E_{CP} + ZPE: interaction energy corrected for counterpoise and zero-point vibrational energy.

indicate the agreement between the computed and experimental values.

4.3.1. ν_3 mode of C_2H_2

As mentioned earlier, the ν_3 stretch of the C_2H_2 submolecule in the complex is observed at 3283.0 cm^{-1}. This value agrees well with the scaled computed value of 3280.3 cm^{-1} for this mode in the complex, as shown in Table 1. The good agreement between the experimental and computed value lends credence to the computationally derived structure of the complex, which is indicated to be of the H–π type, with acetylene being the proton acceptor.

Further, a consideration of the experimentally observed *shifts* in the ν_3 stretch of C_2H_2 submolecule in the complex also supports the computationally predicted structure of the complex. The shift in the ν_3 mode of the C_2H_2 submolecule in the complex is a good indicator of the nature of interaction in the complex. In complexes where acetylene is the proton donor, the shifts in the ν_3 mode of the C_2H_2 submolecule are large. For example, the ν_3 mode of C_2H_2 in the acetylene–water complex is shifted by $\approx$49 cm^{-1}, where the C_2H_2 acts as a proton donor [20]. The small shift (5.9 cm^{-1}) in the ν_3 mode of the C_2H_2 submolecule in the C_2H_2–$CHCl_3$ complex, indicates that C_2H_2 acts as a *proton acceptor* in the complex. The $CHCl_3$ would then be the proton donor in this complex, as also evidenced by the blue shift in the ν_4 mode of the $CHCl_3$ submolecule.

4.3.2. ν_5 mode of C_2H_2.

The ν_5 mode of the C_2H_2 submolecule in the complex, occurs at 743.7 and 748.2 cm^{-1}. As mentioned earlier, the double degeneracy of this mode in free C_2H_2 is split in the complex, as the cylindrical symmetry of C_2H_2 is broken as a result of complex formation. This observation is borne out by our computations, with the scaled computed frequency for this mode in the complex occurring at 741.2 and 747.8 cm^{-1}.

The H–π complex of C_2H_2–$CHCl_3$ can be compared with the H–π complexes of acetylene with hydrogen halides, reported in the literature [22]. The perturbations in the ν_5 mode of C_2H_2 submolecule was larger in the C_2H_2–hydrogen halide complexes than in the C_2H_2–$CHCl_3$ complex. Perturbations in the ν_3 mode of C_2H_2 were not reported in the earlier work to compare the shifts in this mode. While a quantitative correlation cannot be made between the shifts in the vibrational modes of the submoleclules in the complex and the stability of the complex, it can be inferred that the C_2H_2–$CHCl_3$ complex is probably weaker than the complexes of C_2H_2 with hydrogen halides. This trend is of course not surprising given the greater acidities of the hydrogen halides compared with $CHCl_3$.

4.3.3. ν_4 mode of $CHCl_3$

The ν_4 mode of the $CHCl_3$ submolecule was found to be blue shifted by 10.6 cm^{-1} in the complex. Our computations indicate this mode to be blue shifted by $\approx$020 cm^{-1} (Table 1). While our computations and experiments agree on the direction of shift, the computed shifts are almost twice that observed in our experiments. Further, the doubly degenerate ν_4 mode in free $CHCl_3$ is indicated, by our computations, to split in the complex as a result of the lowering of the symmetry. We were, however, able to discern only one of the two components in our spectra.

5. C_2H_2 dimer

In addition to the features assigned to the C_2H_2–$CHCl_3$ complex, we also observed features arising from the existence of C_2H_2 dimer. The features at 3285.2 and 3264.0 cm^{-1} were observed when C_2H_2 alone was deposited in the matrix and the matrix then annealed. These features arise from the C_2H_2 dimer. The experimentally observed features agree well with the computed values for the dimer (Table 1). The feature at 3285.2 cm^{-1} is assigned to the ν_3 mode of the C_2H_2 submolecule in the C_2H_2 dimer, where the C_2H_2 is the proton *acceptor*. The feature near 3265 cm^{-1}, already reported in an earlier matrix isolation work [42], corresponds to the ν_3 mode of the proton *donating* C_2H_2 submolecule. This assignment implies a red shift of 3.7 cm^{-1} in the proton accepting submolecule and a red shift of 24.9 cm^{-1} in the proton donating submolecule. These shifts are consistent with the observation that proton accepting C_2H_2 submolecules show small shifts in this mode, (as in the C_2H_2–$CHCl_3$ complex), while the proton donating C_2H_2 submolecules display large shifts. An earlier gas phase microwave and infrared work had arrived at a

T-shaped structure for the dimer of C_2H_2 and had assigned the transition in the 3271–3274 cm^{-1} region to the ν_3 mode in the proton donating C_2H_2 submolecule [47]. The same article (through a note added in proof) indicated that another transition in the region 3279–3285 cm^{-1} corresponded to the proton accepting C_2H_2 submolecule in the dimer. While the gas phase and the matrix isolated frequencies are different, and not surprisingly so, both studies indicate the proton donating submolecule to have a larger shift than the proton accepting unit.

We also observed features caused by the dimer in the ν_5 bending region of C_2H_2. A feature at 744.9 cm^{-1} appeared when C_2H_2 alone was deposited, and probably belongs to the C_2H_2 dimer. Our computations indicate that this feature, corresponds to the ν_5 mode of the proton accepting C_2H_2 in the dimer (Table 1). Our calculations indicate the ν_5 mode to be split in the dimer and is predicted to occur at 744.9 and 736.4 cm^{-1}. The experimentally observed feature at 744.9 cm^{-1} can be assigned to the higher component of the split doublet in the dimer. The lower frequency component of the split doublet, indicated by our calculations to appear at 736.4 cm^{-1}, is shifted negligibly from the feature of free C_2H_2 and is probably therefore not discerned in our spectra. The features corresponding to the dimer where the C_2H_2 is the proton donor occurs at 757.6 cm^{-1} and is already reported in the literature [42].

The shifts in the ν_3 mode of C_2H_2 in the C_2H_2–$CHCl_3$ and C_2H_2–C_2H_2 are comparable in keeping with the values of experimental gas phase acidities of acetylene and chloroform.

6. Conclusions

We have experimentally observed and computationally proved the existence of a C–H$\cdots\pi$ complex between C_2H_2 and $CHCl_3$, where C_2H_2 acts as a proton *acceptor*. The good agreement between computed and experimental frequencies in the complexes lends credence for the structure predicted by ab initio MO and hybrid density functional calculations. Our computations indicate that in addition to the C–H$\cdots\pi$ interaction in this complex, there also appears to be another stabilization interaction between the H in C_2H_2 and one of the chlorine atoms in the $CHCl_3$. The combined matrix isolation infrared spectroscopy and theoretical studies on 1:1 adduct of acetylene and chloroform give new insights into complexes formed by weakly interacting molecules. The existence of two stabilizing interactions between acetylene and chloroform molecules may serve as a case study encouraging future investigations to look for such possibilities in supermolecules.

In the course of this work, we have also been able to identify features of the acetylene dimer corresponding to the proton donating and proton accepting submolecule. While the assignment for the proton donating submolecule in the dimer exists in the literature, this work has identified features of the proton accepting submolecule. These assignments are corroborated by our computations.

Acknowledgements

We are grateful to the University Grants Commission and the Department of Science and Technology, New Delhi, India for supporting this research. K.T.G. and V.V. gratefully acknowledge research fellowships from the University Grants Commission and the Department of Atomic Energy, respectively. J.L. acknowledges the NSF grant OSR-9452857 and a contract (DAAL 03-89-0038) between the Army Research Office and the University of Minnesota for the Army High Performance Computing Research Center under the auspices of the Department of the Army, Army Research Laboratory cooperative agreement DAAH04-95-2-0003/contract number DAAH04-95-C-008. Neither the policy of the government, nor an official endorsement should be inferred from this article.

References

[1] J.M. Lehn, Supramolecular Chemistry, VCH, Weinheim, 1995.
[2] G.A. Jeffrey, W. Saenger, Hydrogen Bonding in Biological Structures, Springer, Berlin, 1991.
[3] J.L. Atwood, F. Hamada, K.D. Robinson, W.G. Orr, R.L. Vincent, Nature 349 (1991) 683.
[4] D.A. Rodham, S. Suzuki, R.D. Snenram, F.J. Lovas, D. Dasgupta, W.A. Goddard III, G.A. Blake, Nature 362 (1993) 735.

[5] S. Suzuki, P.G. Green, R.E. Bumgarner, D. Dasgupta, W.A. Goddard III, G.A. Blake, Science 257 (1992) 942.
[6] M.A. Viswamitra, R. Radhakrishnan, J. Bandekar, G.R. Desiraju, J. Am. Chem. Soc. 115 (1993) 4868.
[7] I. Rozas, I. Alkorta, J. Elguero, J. Phys. Chem. A 101 (1997) 9457.
[8] K. Kobayashi, Y. Asakawa, Y. Sikuchi, H. Joi, Y. Aoyama, J. Am. Chem. Soc. 115 (1993) 2648.
[9] T. Steiner, J. Chem. Soc. Chem. Commun. (1995) 95, see also references therein.
[10] R. Hunter, R.H. Haueisen, A. Irving, Angew. Chem. Int. Ed. Engl. 33 (1994) 566, see also references therein.
[11] H. Sugimoto, T. Aida, S. Inoue, J. Chem. Soc. Chem. Commun. (1995) 1411.
[12] T. Steiner, E.B. Starikov, A.M. Amado, J.J.C. Teixeira-Dias, J. Chem. Soc. Perkin Trans. 2 (1995) 1321.
[13] T.E. Muler, D.M.P. Mingos, D.J. Williams, J. Chem. Soc. Chem. Commun. (1994) 1787, see also references therein.
[14] M.-F. Fan, Z. Lin, J.E. McGrady, D.M.P. Mingos, J. Chem. Soc. Perkin Trans. (1996) 563.
[15] M. Nishio, M. Hirota, Tetrahedron 45 (1980) 7201.
[16] R.K. McMullan, Å. Kvick, P. Popelier, Acta Crystallogr. Sect. B 48 (1992) 726.
[17] T.E. Müller, D.M.P. Mingos, D.J. Williams, J. Chem. Soc. Chem. Commun. (1994) 1787.
[18] G.T. Frazer, F.J. Lovas, R.D. Suenram, J.Z. Gillies, C.W. Gillies, Chem. Phys. 163 (1992) 91.
[19] R. Hunter, R.H. Haueisen, A. Irving, Angew. Chem. Int. Ed. Engl. 33 (1994) 566.
[20] A. Endahl, B. Nelander, Chem. Phys. Lett. 100 (1983) 129.
[21] H. Jeng Mei-Lee, B. S. Ault, J. Phys. Chem. 94 (1990) 1323.
[22] S.A. McDonald, G.L. Johnson, B.W. Keelan, L. Andrews, J. Am. Chem. Soc. 102 (1980) 2892.
[23] A. Engdahl, B. Nelander, Chem. Phys. Lett. 113 (1985) 49.
[24] L. Andrews, G.L. Johnson, B.J. Kelsall, J. Am. Chem. Soc. 104 (1982) 6180.
[25] L. Andrews, G.L. Johnson, B.J. Kelsall, J. Chem. Phys. 76 (1982) 5767.
[26] F.A. Balocchi, J.H. Williams, W. Klemperer, J. Phys. Chem. 87 (1983) 2079.
[27] A. Engdahl, B. Nelander, J. Phys. Chem. 89 (1985) 2860.
[28] L. Andrews, G.L. Johnson, S.R. Davis, J. Phys. Chem. 89 (1985) 1706.
[29] A. Engdahl, B. Nelander, J. Phys. Chem. 91 (1987) 2253.
[30] R.D. Hunt, L. Andrews, J. Phys. Chem. 96 (1992) 6945.
[31] L. George, K. Sankaran, K.S. Viswanathan, C.K. Mathews, Spectrochim. Acta. 51A (1995) 587.
[32] L. George, K. Sankaran, K.S. Viswanathan, C.K. Mathews, Appl. Spectrosc. 48 (1994) 7.
[33] M.J. Frisch, G.W. Trucks, M. Head-Gordon, P.M.W. Gill, M.W. Wong, Foresman, B.G. Johnson, H.B. Schlegel, M.A. Robb, E.S. Replogle, R. Gomperts, J.L. Andres, K. Raghavachari, J.S. Binkley, Gonzalez, R.L. Martin, D.J. Fox, D.J. Defrees, J. Baker, J.J.P. Stewart, J.A. Pople, GAUSSIAN 92, Revision A, Gaussian, Inc., Pittsburgh, PA, (1992).
[34] M.J. Frisch, G.W. Trucks, H.B. Schlegel, P.M.W. Gill, B.G. Johnson, M.A. Robb, J.R. Cheeseman, T. Keith, G.A. Petersson, J.A. Montgomery, K. Raghavachari, M.A. Al-Laham, V.G. Zakrzewski, J.V. Ortiz, J.B. Foresman, J. Cioslowski, B.B. Stefanov, A. Nanayakkara, M. Challacombe, C.Y. Peng, P.Y. Ayala, W. Chen, M.W. Wong, J.L. Andres, E.S. Replogle, R. Gomperts, R.L. Martin, D.J. Fox, J.S. Binkley, D.J. Defrees, J. Baker, J.J.P. Stewart, M. Head-Gordon, Gonzalez, J.A. Pople, GAUSSIAN 94, Revision D.1, Gaussian, Inc., Pittsburgh, PA, (1995).
[35] C. Moller, M.S. Plesset, Phys. Rev. 46 (1934) 618.
[36] A.D. Becke, Phys. Rev. A 38 (1988) 3098.
[37] A.D. Becke, J. Chem. Phys. Phys. Rev. 98 (1983) 5648.
[38] C. Lee, W. Yang, R.G. Parr, Phys. Rev. B 37 (1988) 785.
[39] P.J. Stephens, F.J. Delvin, C.F. Chabalowski, M.J. Frisch, J. Phys. Chem. 98 (1994) 11623.
[40] W.J. Hehre, L. Radom, P.V.R. Schleyer, J.A. Pople, Ab Initio Molecular Orbital Theory, Wiley, New York, 1986.
[41] S.F. Boys, F. Bernardi, Mol. Phys. 19 (1970) 553.
[42] E.S. Kline, Z.H. Kafafi, R.H. Hauge, J.L. Margrave, J. Am. Chem. Soc. 107 (1985) 7559.
[43] O. Navon, J. Bernstein, V. Khodorkovsky, Angew. Chem. Int. Ed. Engl. 36 (1997) 601.
[44] H. Dadon, J. Bernstein, Inorg. Chem. 36 (1997) 2898.
[45] K. Zhang, E.G. Lewars, R.E. March, J.M. Parnis, J. Phys. Chem. 97 (1993) 4320.
[46] S.W. Han, K. Kim, J. Phys. Chem. 100 (1996) 17124.
[47] D.G. Prichard, R.N. Nandi, J.S. Muenter, J. Chem. Phys. 89 (1988) 115.